Superhigh-frequency surface-acoustic-wave transducers using AlN layers grown on SiC substrates

Y. Takagaki,[a] P. V. Santos, E. Wiebicke, O. Brandt, H.-P. Schönherr, and K. H. Ploog
Paul-Drude-Institut für Festkörperelektronik, Hausvogteiplatz 5-7, 10117 Berlin, Germany

(Received 6 June 2002; accepted for publication 31 July 2002)

We demonstrate the operation of surface-acoustic-wave (SAW) transducers fabricated on AlN/SiC structures at frequencies as high as 19 GHz. The high SAW velocity of the AlN film is enhanced by the even higher sound velocity of the SiC substrate, enabling us to achieve these frequencies with a SAW wavelength of 400 nm. © *2002 American Institute of Physics*. [DOI: 10.1063/1.1509471]

Surface acoustic waves (SAWs) propagating on the surface of a piezoelectric material have a variety of applications in signal processing and nondestructive material characterization. In the former case, devices based on SAW excitation and detection such as delay lines, resonators, convolvers, and filters are vital components particularly in telecommunication. The everlasting demand to increase the transmission frequency requires these devices to operate at higher frequencies.

A straightforward way to raise the operating frequency of SAW transducers is to use materials having large sound velocities. Efforts have been made in this respect to establish processes to construct SAW devices using diamond,[1,2] GaN,[3,4] or AlN,[3,5] which are among the materials with the highest sound velocities. Owing to the recent remarkable progress in the growth of GaN and AlN layers, these materials can now be provided with sufficiently high crystal quality to utilize their potential for high frequency applications.

In this letter, we report the operation of SAW transducers at frequencies as high as 19 GHz using AlN films grown on SiC substrates. While SAW frequencies up to 17 GHz have been achieved using interdigital transducers (IDTs) on $LiNbO_3$,[6] the highest frequency reported so far for AlN-based transducers is below 2 GHz.[3,5] The increase by more than one order of magnitude is accomplished by the use of SiC substrates and electron-beam lithography.

We have chosen to exclusively employ AlN in our experiments as AlN is superior to GaN for SAW devices for the following reasons. First, SAWs propagate faster in AlN than in GaN (the SAW velocity is 5790 m/s in AlN and 3693 m/s in GaN). Second, GaN frequently exhibits a considerable background carrier density at room temperature, whereas AlN is insulating in nature. Free carriers are problematic as they short-circuit the bias voltage applied to the IDTs and screen the SAW-generated piezoelectric fields, thereby reducing simultaneously the generation and the detection efficiencies.

The AlN films were grown on semi-insulating 4H-SiC(0001) substrates by plasma-assisted molecular-beam epitaxy at a substrate temperature of 800 °C, a plasma power of 180 W, and a N_2 flow of 1 sccm, yielding a nitrogen-limited growth rate of 0.25 μm/h. Growth was monitored *in-situ* by reflection high-energy electron diffraction. The effective surface stoichiometry was adjusted to be as close to unity as possible, exploiting the recovery of the reflection high-energy electron diffraction intensity upon growth interruptions analogous to our procedure for GaN.[7] As a result, the films exhibited smooth surfaces with typical values for the peak-to-valley roughness of 5 to 15 nm and for the rms roughness of 0.5 to 2 nm. The width of the (0002) x-ray rocking curve as measured by double crystal x-ray diffractometry amounted to 200 to 400″. All samples were highly resistive.

The IDTs were processed on the epitaxial layers using electron-beam lithography and the lift-off technique. The single-finger metal gates of the IDTs consist of a 6-nm-thick Ti film and a 25-nm-thick Al film. We note that AlN is lighter than, for example, GaAs, giving rise to a less significant proximity effect during the lithography. The SAW delay lines were fabricated by aligning two identical transducers along the $[1\bar{1}00]$ crystallographic direction. This direction was chosen solely because it is one of the cleavage directions of the crystal (the SAW propagation is isotropic in the *c*-plane of AlN and SiC). The distance between the transducers was 500 μm, and the transmission and reflection characteristics of the delay lines were evaluated using an HP 8720D network analyzer.

We have fabricated IDTs of various geometrical sizes. All of them functioned reasonably well, benefiting from the fairly large electromechanical coupling coefficient of AlN.[8] To highlight the capability of operation at extremely high frequencies, we show results from two devices, of which the structural parameters are summarized in Table I.

When the SAW wavelength λ_{SAW} is larger than the thickness *d* of the AlN film, the dominant SAW transmission is due to the first-order Rayleigh mode, which is the normal SAW mode in piezoelectric materials. The SAW velocity of

TABLE I. Geometrical sizes of the single-finger interdigital transducers.

	Delay line	
	#1	#2
Thickness of AlN film, *d* (μm)	1	0.25
SAW wavelength, λ_{SAW} (nm)	435	400
Aperture (μm)	52	30
Number of finger pairs	160	100

[a]Electronic mail: takagaki@pdi-berlin.de

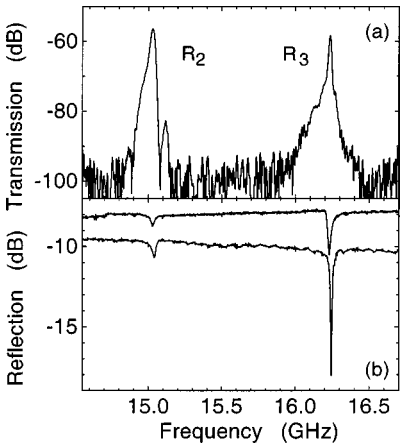

FIG. 1. (a) Transmission and (b) reflection characteristics of delay line #1. The resonances labeled R_2 and R_3 are associated with the second- and third-order Rayleigh modes, respectively.

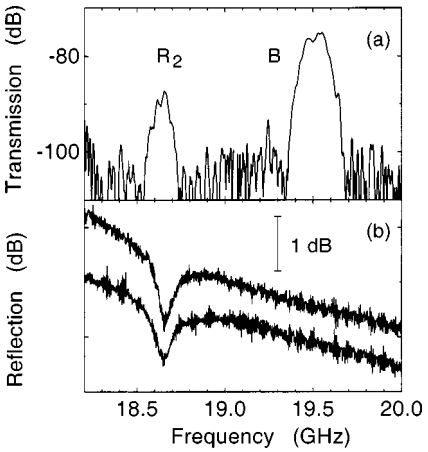

FIG. 2. (a) Transmission and (b) reflection characteristics of delay line #2. The resonance labeled R_2 is associated with the second-order Rayleigh mode. The transmission peak labeled B originates from the scattering of acoustic waves from the sample edge. The curves in (b) are vertically offset for clarity.

this mode changes from that of SiC to that of AlN with decreasing λ_{SAW}, as the SAWs are localized in the immediate vicinity of the surface over a distance of about one wavelength. In the present materials system, the SAW velocity of the substrate (6832 m/s) is larger than that of the epitaxial film. The acoustic waves are thus reflected from the fast-velocity substrate. Under this circumstance, higher-order Rayleigh modes emerge when λ_{SAW} is reduced to be smaller than d. The higher-order Rayleigh modes can be regarded as the higher-order "transverse modes" in the AlN waveguide.[9,10]

In Figs. 1(a) and 1(b), we show, respectively, the transmission and reflection amplitude in delay line #1, which was defined on a 1-μm-thick AlN film. Two clear resonances are observed in both spectra. As λ_{SAW} ($=435$ nm)$\ll d$, the transmission resonances at 15.03 and 16.24 GHz turn out to be mediated by the second-order (R_2) and third-order (R_3) Rayleigh modes, respectively.

To confirm this assignment of the SAW modes, we have carried out numerical simulations of the SAW propagation in AlN/SiC structures. The parameters used for the calculation are given in Table II. For the experimental condition of $\lambda_{SAW}/d=0.435$, the velocities of the R_2 and R_3 modes are determined to be 6494 and 7101 m/s, respectively. These theoretical values are in good agreement with the experimental values of 6534 and 7060 m/s. We emphasize that these velocities are even larger than the SAW velocity of SiC. The SAW velocities increase with increasing order of the Rayleigh mode. (The SAW velocity of the first-order (R_1) Rayleigh mode when $\lambda_{SAW}/d=0.435$ is estimated to be 5791 m/s.) Thus, higher-order Rayleigh modes are advantageous for high-frequency IDTs.

Delay line #2 was prepared on a 250-nm-thick AlN film. The transmission characteristic of this device is displayed in Fig. 2(a). The transmission resonance at the frequency of 18.65 GHz is due to the R_2 Rayleigh mode. The calculated velocity of the R_1 mode is 5998 m/s when $\lambda_{SAW}/d=1.6$. Examining the transmission properties for various values of λ_{SAW}, we have found that, on the one hand, the transmission amplitude associated with the R_1 mode for $d=250$ nm is below the detection limit (~ -100 dB) when λ_{SAW} is smaller than 700 nm. On the other hand, the R_2 mode becomes sufficiently strong to be detected only when λ_{SAW} is as small as 400 nm. Consequently, no SAW transmission was observed when 700 nm$>\lambda_{SAW}>$400 nm.

TABLE II. Mass density ρ (in unit of kg/m^3) and elastic constants c_{ij} (in units of 10^{12} N/m^2) used for the calculations.

	ρ	c_{11}	c_{12}	c_{13}	c_{33}	c_{44}	c_{66}
AlN	3230	0.41	0.14	0.1	0.39	0.12	0.135
SiC	3211	0.507	0.108	0.0558	0.547	0.17	0.1995

The resonance frequency implies that the velocity of the R_2 mode is 7456 m/s. The transverse bulk velocity of SiC with polarization parallel to the c-axis is predicted to be $v_{T_1}=\sqrt{c_{44}/\rho}=7276$ m/s. This velocity sets the upper limit for non-leaky Rayleigh modes. From the calculation, we do not expect non-leaky R_2 Rayleigh mode when $\lambda_{SAW}/d=1.6$. Nevertheless, extrapolating the numerical results for small λ_{SAW} yields a velocity that is in good agreement with the experimental value. The leaky nature of the mode is likely to be responsible for the large insertion loss. We thus expect the insertion loss to decrease when λ_{SAW} is further reduced since the velocity of R_2 mode becomes smaller than v_{T_1}. However, we are at present unable to confirm this speculation, as the corresponding resonance frequencies exceed the upper limit of our measurement equipment.

The spectrum in Fig. 2(a) exhibits an even stronger transmission, labeled B, at 19.5 GHz. However, unlike the Rayleigh modes, no corresponding resonance is found in the reflection spectrum, as can be seen in Fig. 2(b). To clarify this situation, we have examined the transmission properties among three identical IDTs. The impulse response of the delay line can be obtained by Fourier-transforming the transmission spectrum. The propagation time between the IDTs determined in this manner, shown in Fig. 3(a), varies in accordance with the distance of the delay line from the sample edge [the IDTs are arranged in the way illustrated in the inset of Fig. 3(b)]. This finding strongly suggests that the transmission peak B originates from reflection from the sample boundary. Curiously, the peak frequency of this mode is found to depend on the separation between the delay line and

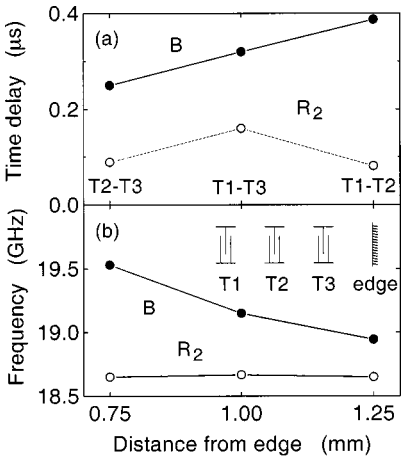

FIG. 3. (a) Time delay for the propagation between the IDTs and (b) position of the transmission peak in frequency vs the distance from the center of the delay line to the sample edge. The filled and open circles correspond to the modes B and R_2, respectively. Higher-order transmission peaks in the time domain due to multiple reflections are not included. The inset in (b) shows the configuration of the three IDTs (T1, T2, and T3) with respect to the sample edge. The separation between the adjacent IDTs and that between the IDT T3 and the sample edge are both 500 μm. The combination of the IDTs for the transmission measurements is indicated in (a).

the sample edge as shown in Fig. 3(b), while the resonance frequency of the R_2 mode is, as expected, independent of the distance. We believe that interference effects may play an important role for these anomalous properties of the transmission mode B.

In conclusion, we have fabricated IDTs having a period of about 400 nm using electron-beam lithography on AlN films grown on SiC substrates. SAW transmission between the IDTs has been confirmed at a frequency as high as 19 GHz. Using higher-order Rayleigh modes, we have shown that SAW velocities even higher than those of AlN and SiC can be reached.

Part of this work was supported by the Deutsche Forschungsgemeinschaft and by the NEDO collaboration program.

[1] H. Nakahata, K. Higaki, A. Hachigo, S. Shikata, N. Fujimori, Y. Takahashi, T. Kajiwara, and Y. Yamamoto, Jpn. J. Appl. Phys. **33**, 324 (1994).
[2] H. Nakahata, H. Kitabayashi, T. Uemura, A. Hachigo, K. Higaki, S. Fujii, Y. Seki, K. Yoshida, and S. Shikata, Jpn. J. Appl. Phys. **37**, 2918 (1998).
[3] C. Deger, E. Born, H. Angerer, O. Ambacher, M. Stutzmann, J. Hornsteiner, E. Riha, and G. Fischerauer, Appl. Phys. Lett. **72**, 2400 (1998).
[4] A. Khan, R. Rimeika, D. Ciplys, R. Gaska, and M. S. Shur, Phys. Status Solidi B **216**, 477 (1999).
[5] H. Okano, N. Tanaka, Y. Takahashi, T. Tanaka, K. Shibata, and S. Nakano, Appl. Phys. Lett. **64**, 166 (1994).
[6] K. Yamanouchi, T. Meguro, Y. Wagatsuma, H. Odagawa, and K. Yamamoto, Jpn. J. Appl. Phys., Part 1 **33**, 3018 (1994).
[7] O. Brandt, R. Muralidharan, P. Waltereit, A. Thamm, A. Trampert, H. von Kiedrowski, and K. H. Ploog, Appl. Phys. Lett. **75**, 4019 (1999).
[8] D. Ciplys, R. Rimeika, M. S. Shur, S. Rumyantsev, R. Gaska, A. Sereika, J. Yang, and M. A. Khan, Appl. Phys. Lett. **80**, 2020 (2002).
[9] E. H. El Boudouti, B. Djafari-Rouhani, and A. Akjouj, Phys. Rev. B **55**, 4442 (1997).
[10] X. Zhang, J. D. Comins, A. G. Every, P. R. Stoddart, W. Pang, and T. E. Derry, Phys. Rev. B **58**, 13677 (1998).